Seakeeping of Recycled Plastic Jerry Can - Based Pontoon Floating Rigid Dock for Estuary Area Application

G. A. P. Poundra[ab*], R. Sitepu[b], S. Widiyanto[a], B.K. Aditya[a], H. Suyanto[a]
[a] *Hang Tuah University, Jl. Arif Rahman Hakim No. 150, Surabaya 60111, Indonesia*
[b] *Universitas Katolik Widya Mandala Surabaya, Jl. Dinoyo No. 42-44, Surabaya 60265*
Corresponding author: prabhawatya.poundra@hangtuah.ac.id

Abstract

Floating docks provide essential infrastructure for transportation, fisheries, and community activities in estuarine environments, where fluctuating water levels and limited port facilities require stable, economical, and sustainable floating structures. This study investigates the hydrostatic characteristics and seakeeping performance of modular floating rigid dock configurations utilizing recycled 30-L high-density polyethylene (HDPE) plastic jerry cans as buoyancy modules. Three configurations, namely the Base, T-shaped, and U-shaped models, were numerically evaluated using Maxsurf Modeler and Maxsurf Motions under irregular JONSWAP wave conditions. The hydrostatic analysis revealed that the T-shaped and U-shaped configurations increased displacement by approximately 44.3% and 122.3%, respectively, compared with the Base model, while the U-shaped configuration achieved the highest transverse metacentric height (GMt = 2.144 m**).** Frequency-domain seakeeping analysis showed that the heave and pitch responses of all configurations remained comparable, with differences generally below 10%**,** indicating that changes in pontoon arrangement had minimal influence on vertical motion characteristics under moderate wave conditions. In contrast, the T-shaped configuration reduced the peak roll response amplitude operator (RAO) by approximately 23% compared with the U-shaped configuration, demonstrating improved transverse motion performance while maintaining comparable heave and pitch responses. Considering hydrostatic capacity, operational stability, structural functionality, and site adaptability, the T-shaped configuration exhibited the most balanced overall performance for estuarine floating dock applications. These findings demonstrate that recycled HDPE plastic jerry cans can serve as technically feasible, sustainable, and low-cost buoyancy modules for modular floating dock systems.

Keywords: Seakeeping; Floating Rigid Dock; Estuary; Recycled Plastic Jerry Can – Based Pontoon; Maxsurf: Motions

1. Introduction

Floating rigid dock systems play an important role in supporting small-vessel operations, fisheries activities and community-based maritime transportation in coastal and estuarine regions. Unlike fixed piers, floating rigid docks can adapt to tidal fluctuations and variations in water level, making them particularly suitable for shallow water environments and areas vulnerable to flooding [1] [2]. Their relatively simple construction and ease of installation have led to widespread adoption in small harbors, fishing villages and river-mouth settlements [3] [4]. Despite these advantages, conventional floating rigid dock systems commonly rely on commercially manufactured pontoons made of steel, aluminum, fiberglass, or high density polyethylene (HDPE). While these materials provide adequate buoyancy and durability, their acquisition and maintenance costs can be prohibitively expensive for small coastal communities in developing countries. Furthermore, the production of new pontoon materials requires considerable energy and resources, such as high skilled labors and sophisticated manufacturing facilities, creating additional environmental burdens throughout their life cycle [5] [6].

In parallel with these challenges, plastic waste management has become a major environmental concern worldwide [7] [8]. Large quantities of plastic containers, including jerry cans used for industrial, domestic and transportation purposes, are discarded after reaching the end of their primary service life. Although recycling programs have expanded in many regions, a significant proportion of plastic waste continues to accumulate in landfills, waterways, and coastal environments, contributing to long-term ecological degradation [9] [10]. Reusing discarded plastic jerry cans as buoyancy modules for floating structures offers a practical circular-economy solution by extending material service life while simultaneously reducing construction costs and environmental impacts.

Several studies have investigated the hydrostatic and hydrodynamic performance of floating structures, including floating platforms, pontoons, and offshore facilities. However, most previous investigations have focused on conventional pontoon materials and ship-shaped floating bodies [2] [4] [1]. Research specifically addressing floating rigid dock systems remains relatively limited, particularly for configurations employing recycled plastic jerry cans as primary buoyancy elements. More importantly, the influence of dock geometry on the seakeeping performance of

Received: May 18, 2026
Accepted: July 14, 2026
DOI: 10.12962/j28075064.v12i1.9750

recycled-plastic-based floating docks under irregular wave conditions has not been adequately examined in the existing literature.

The absence of hydrodynamic assessment represents an important knowledge gap because floating docks are continuously subjected to environmental loads generated by waves, currents, and tidal fluctuations. Excessive motions reduce operational safety, passenger comfort, and docking effectiveness. Therefore, understanding the seakeeping characteristics of alternative pontoon systems is essential before their practical implementation in estuarine environments.

The novelty of this study lies in the numerical investigation of floating rigid dock configurations utilizing recycled plastic jerry cans as buoyancy modules and the evaluation of their seakeeping performance under irregular wave conditions represented by the JONSWAP spectrum. Three dock configurations, namely Base model, U-Shaped and T-Shaped models, are compared through hydrostatic and frequency-domain seakeeping analyses using Maxsurf Modeller and Maxsurf Motions. The study aims to identify the most suitable configuration for estuarine applications while simultaneously demonstrating the technical feasibility and environmental benefits of recycled plastic jerry cans as sustainable pontoon materials for low-cost floating dock systems.

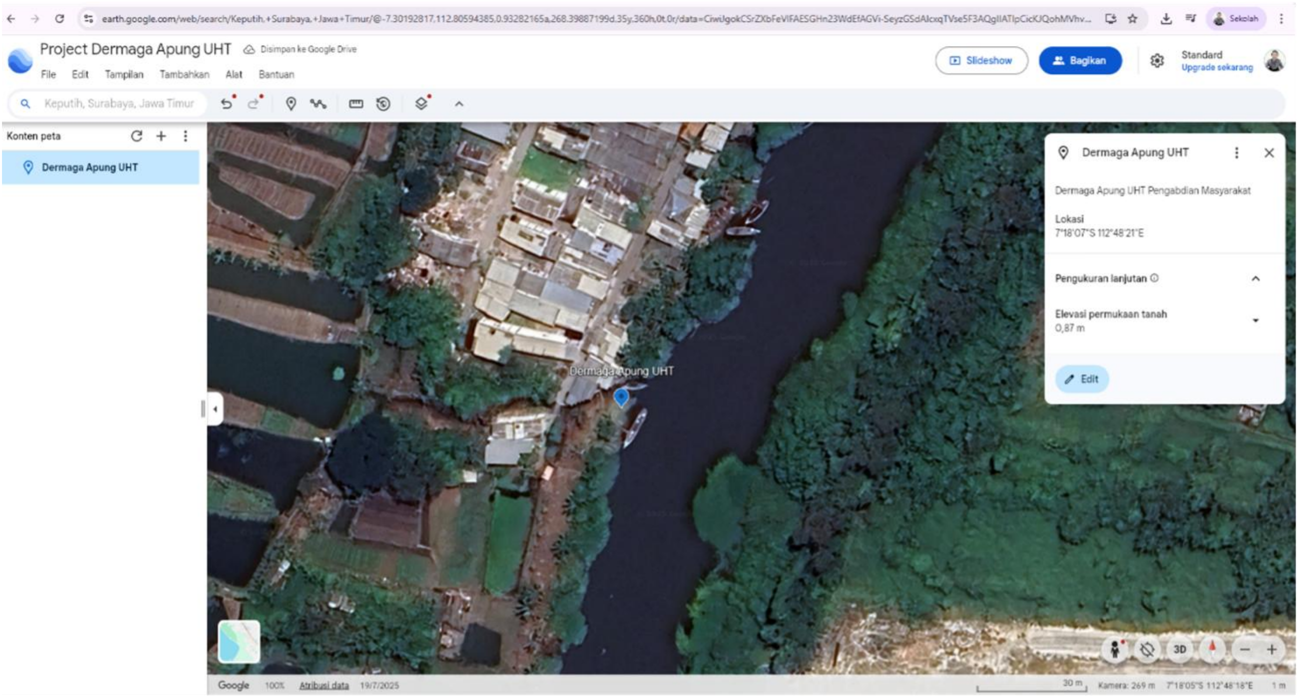

Figure 1. Field Data Measurement Location

In this research, a small fishing village located in East Java, Indonesia was taken to be the sample. This village located near the Jagir River bank (belongs to Wonokromo canal) which can be seen in Figure 1. Looking at the situation of the village, this place can be very sensitive to tidal flooding and erosion as the residential area situated too close to the river bank [11] [12]. Thus, in order to help them to live in such risky place, floating rigid dock as a multi-purpose platform with functions which may covered the needs of people who live near the coastal areas, such as boat docking platform, a place where the tidal and sea level rise sensor and instruments can be placed, as well as a hub for the coastal communities [4] [13]. Besides that, floating rigid dock can be built using simple materials which can be found around us without involving expensive or sophisticated things. Moreover, its simple hull form also makes the building process simpler and bringing an advantage for people who do not having any basic in engineering (especially marine or naval engineering) to build it with ease [1] [14] [15].

Nomenclature

λ	: Wavelength
k	: Wave number
A	: Amplitude
ω	: Angular Velocity
ω_0	: Initial Angular Velocity
h	: Wave Height
r	: Wave Gyration Radius

$S(\omega)$: Wave Spectra
T : Wave Period
f : Wave Frequency
φ : Wave Phase
ζ : Wave Elevation
V_w : Wave Velocity
p : Pressure
E_k : Kinetic Energy
z : Depth
E_p : Potential Energy
ε : Phase Angle
σ_M : Wave slope
∇ : Volume Displacement
c : Wave Coefficient
$H_{1/3}$: Wave Height Based on Pierson-Moskowitz
g : Gravitational Acceleration
WSA : Wetted-Surface Area
WPA : Water-Plane Area
C_b : Block Coefficient
C_P : Prismatic Coefficient
C_{WP} : Water-plane Coefficient
C_m : Midship Coefficient
Lwl : Length of Water Line
WL : Water Line
LCB : Longitudinal Centre of Buoyancy
LCF : Longitudinal Centre of Floatation
d/T : Draught
Cm : Midship Coefficient
MTc : Moment to Change Trim by 1 cm
TPc : Tonne per cm^3
KG : Keel to Centre of Gravity (Vertical Centre of Gravity (VCG))
KB : Keel to Centre of Buoyancy (Vertical Centre of Buoyancy (VCB))
BMt : Metacentric Radius Transversal
BML : Metacentric Radius Longitudinal
GMt : Metacentric Height Transversal
GML : Metacentric Height Longitudinal
V_S : Ship Service Speed
V_a : Ship Maximum Speed

2. Method

Although many engineers have successfully built floating rigid docks, its engineering analyses and reviews (both hydrodynamically and structural strength) in different environmental conditions with their unique phenomena remains interesting to be acknowledged. In this research, the hydrodynamic performance of several floating rigid docks models was calculated based on seakeeping criteria using Maxsurf: Motions engineering software [15] [16]. The software was used to calculate the behavior of the platform when interacted with waves, wind and surface current based on the water area characteristics [17]. This engineering software was a simple user interface software utilized to calculate ship performance, such as resistance, stability, seakeeping and structure. The use of this software to fasten the process of engineering calculation and analysis considering floating rigid dock is a simple platform which does not requires a sophisticated mathematical model to calculate its performance [18].

2.1. Floating Rigid Dock Configurations

The geometric modeling of a floating rigid dock in Maxsurf begins with establishing a NURBS-based computational domain in which the principal dimensions are permanently defined. A rectangular surface patch is generated, typically representing half of the dock's transverse geometry to exploit symmetry about the centerline. Control points are assigned precise Cartesian coordinates to ensure that the surface accurately represents the intended boundary conditions, forming the initial approximation of the dock's hull envelope. Subsequent refinement of the geometry involves systematic manipulation of the surface's control net to achieve the desired hydrostatic form. The upper control-point row is elevated to define the freeboard and deck plane, while the lower row is aligned with the keel baseline to establish the submerged boundary. The lateral control points are adjusted to produce vertical or chamfered sides, ensuring geometric continuity and avoiding surface twist. Additional NURBS surfaces may be introduced to represent internal bulkheads or compartmental subdivisions, improving the fidelity of the model for later seakeeping analyses. Fairness evaluation tools, such as curvature analysis and sectional slicing, are applied to validate the smoothness and physical plausibility of the resulting hydrodynamic surfaces.

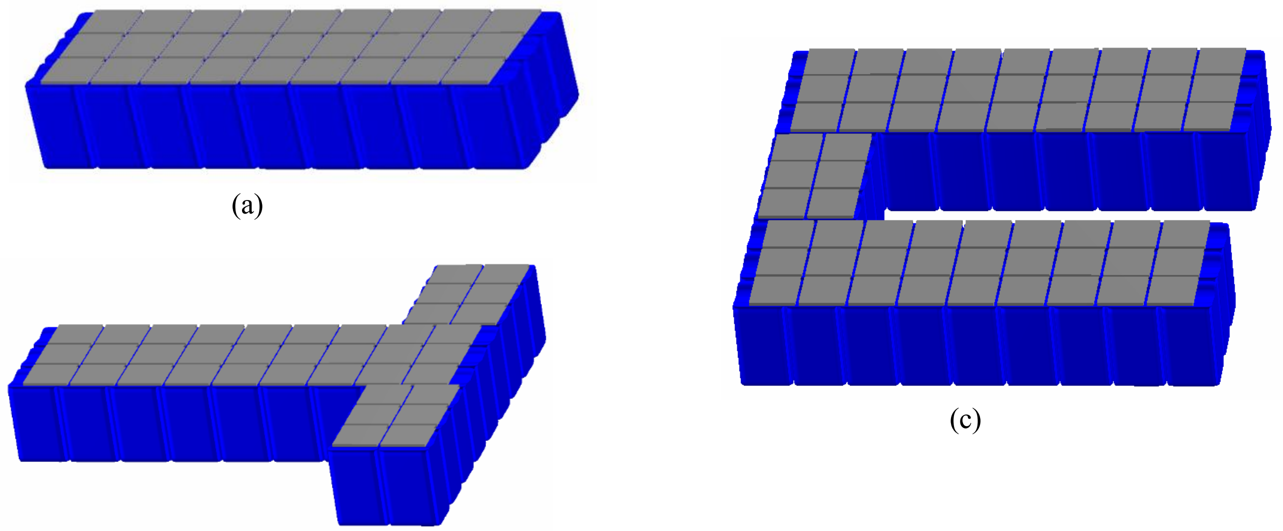

(a)

(b)

(c)

Figure 2. 3D Models of Floating Rigid Dock

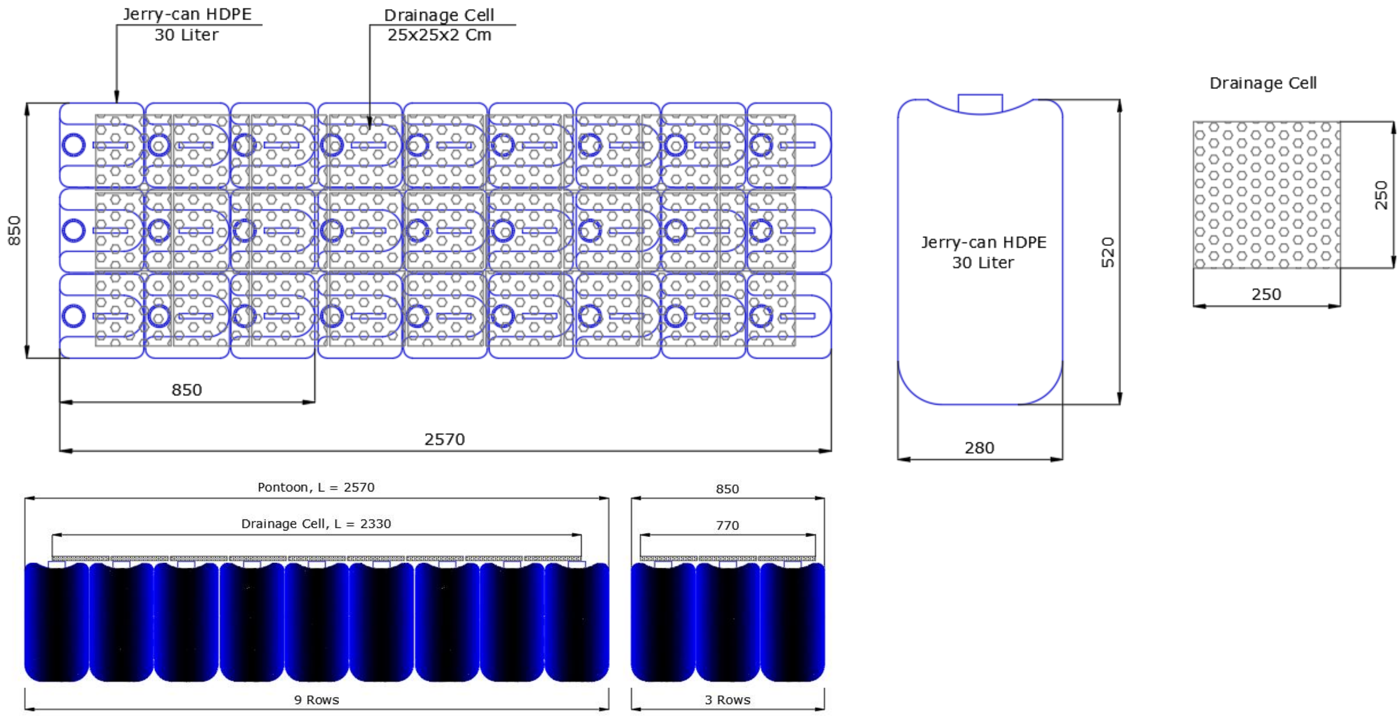

Figure 3. Floating Rigid Dock Base Model Layout

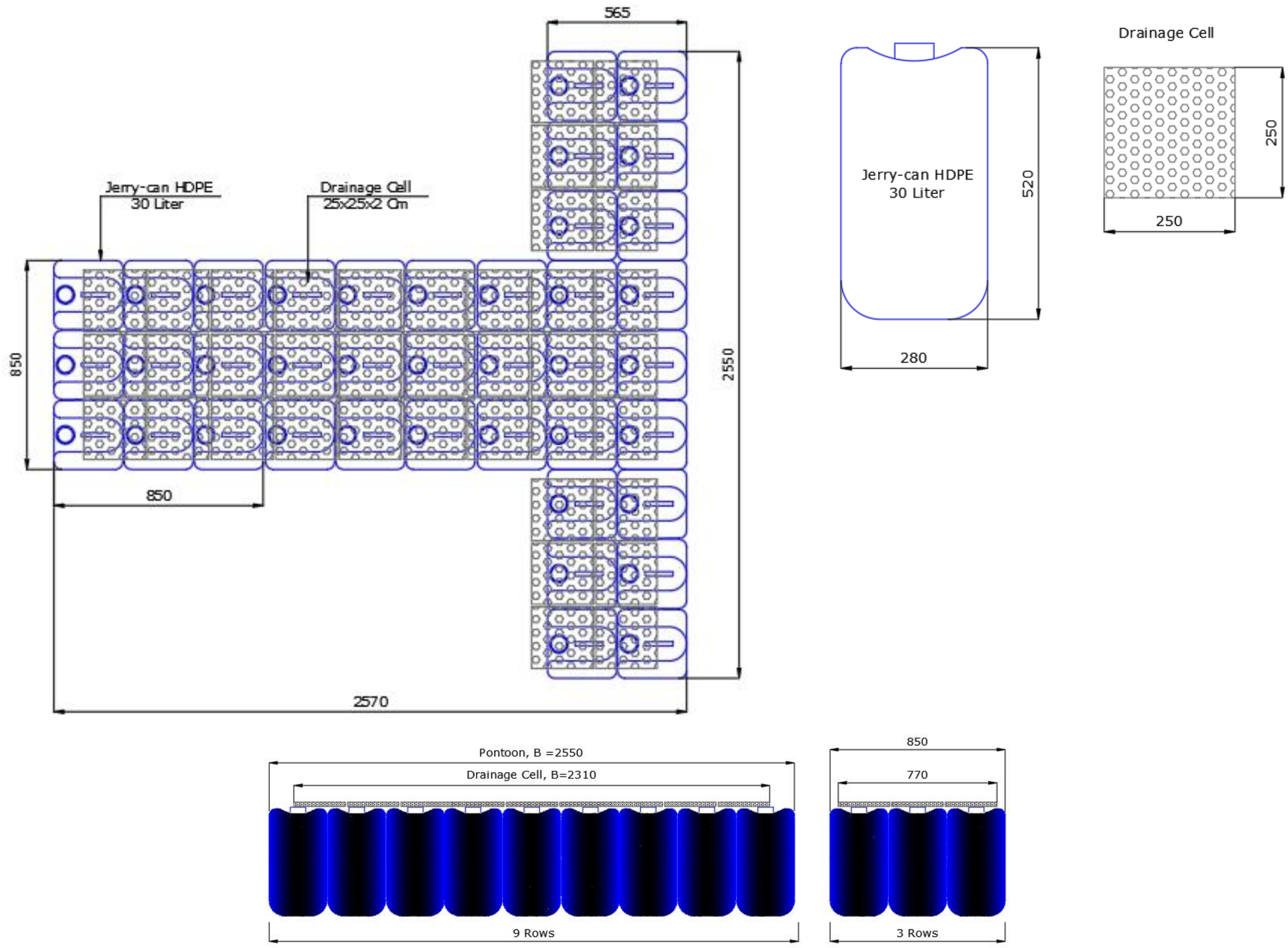

Figure 4. Floating Rigid Dock T-Shape Model Layout

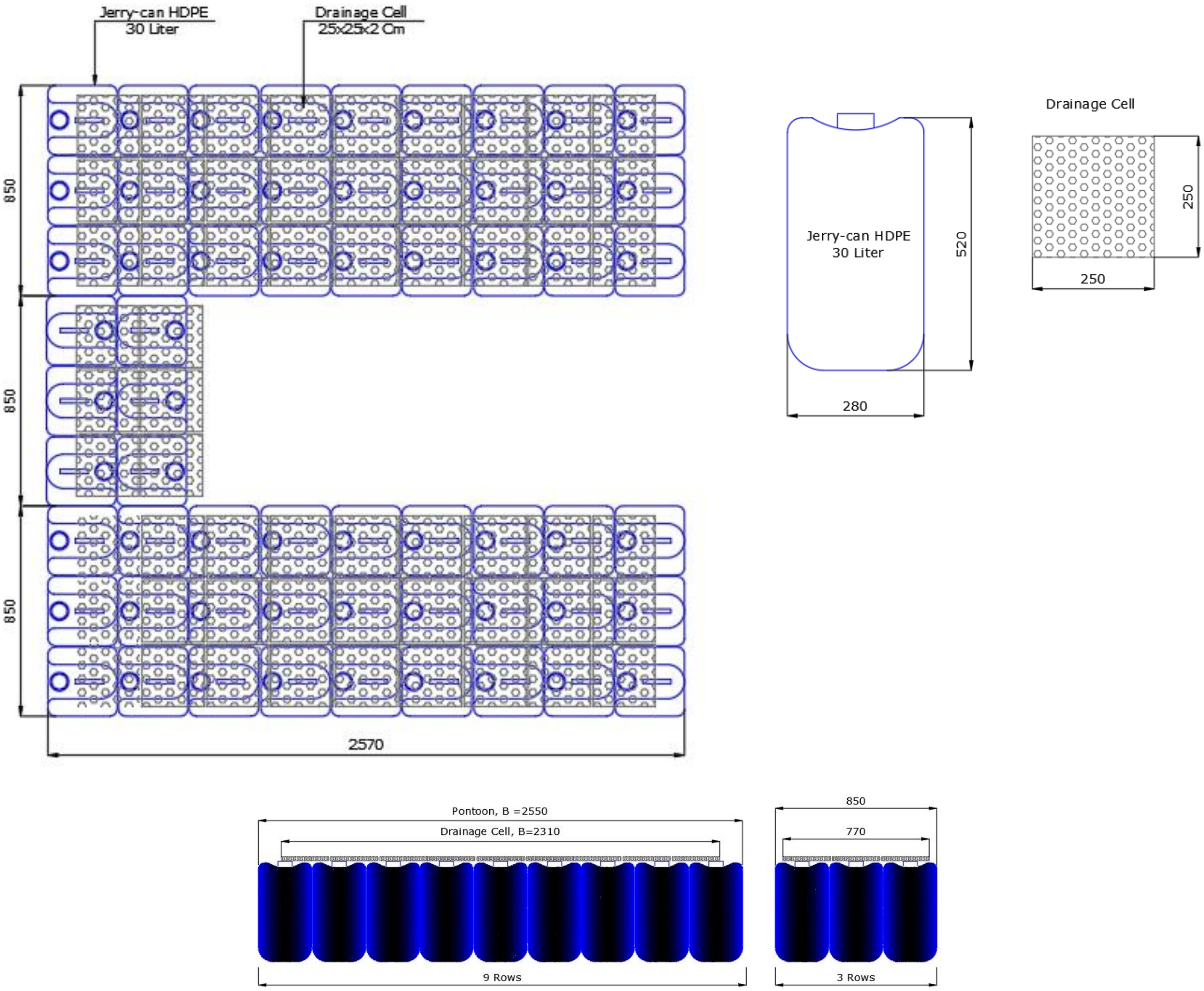

Figure 5. Floating Rigid Dock U-Shape Model Layout

2.2. Seakeeping Analysis

The preliminary phase of a seakeeping analysis commences with a comprehensive site characterization encompassing geographical identification, in-situ observations, hydrodynamic profiling and the definition of operational performance requirements. This phase typically involves high-resolution bathymetric surveying and the quantitative assessment of key metocean parameters – namely tidal oscillations, directional wave spectra, depth – dependent current velocity fields, and local wind climatology – to establish the environmental loading conditions that will govern the structural and hydrodynamic response of the dock system [19] [20]. Field observations indicate the wave propagation within the study area is predominantly unidirectional, corresponding with the alignment of the surface currents along the river flow. Under these conditions, the dock is primarily subjected to three rigid-body motions induced by wave – current interactions, namely: heave, pitch and roll [21].

Based on the condition found in the field observations, two different angles of attacks were chosen to simulate the inlet waves of the fluid flow, i.e. 180^o, and 90^o with settings that might resembling the irregular waves. The spectrum of the wave in this analysis was using the Joint North Sea Wave Project (JONSWAP) to describe the distribution of energy with frequency in a developing wind-generated water area, in this case, estuary [22].

The numerical simulations were performed using the following environmental parameters obtained from field observations:

Table 1. Environment Condition Data

Parameters	**Value**	**Unit**
Water Depth	2.00	m
Significant Wave Height	0.2	m
Peak Wave Period	15.71 ~ 0.35	s
Wave Heading Angle	90 and 180	Degree
Wave Frequency Range	0.4 ~ 18	rad/s

The seakeeping simulations were performed using Maxsurf Motions, which applies linear strip theory in the frequency domain based on potential flow assumptions. Hydrodynamic coefficients, including added mass, damping, and wave excitation forces, were generated internally by the software as functions of encounter frequency. Unlike CFD-based approaches, the method does not require computational mesh generation or mesh independence verification. The analysis was conducted using the environmental conditions obtained from field observations, including wave heading angle, water depth, and wave spectrum characteristics represented by the JONSWAP formulation. Mathematically the spectra model can be expressed as follows [18]:

$$S_j(\omega) = \frac{ag^2}{\omega^5} exp\left[-\frac{5}{4}\left(\frac{\omega_p}{\omega}\right)^4\right]\gamma^r \tag{1}$$

On the other hand, heave, pitch and roll motion which can be triggered by the wave – structure interaction in water area condition as such, mathematically can be expressed as [19]:

$$a\ddot{z} + b\dot{z} + cz = F_0 \cos \omega_e t \tag{2}$$

$$d\ddot{\theta} + e\theta + h\theta = M_0 \cos \omega_e t \tag{3}$$

$$\alpha \frac{d\phi}{dt} + \alpha \frac{d\phi}{dt} + c\phi = M_0 \cos \omega_e t \tag{4}$$

In addition to the governing equations typically employed in seakeeping analysis, particular emphasis is placed on the Response Amplitude Operator (RAO), a fundamental descriptor of a vessel's dynamic behavior in waves. The RAO is formally defined as the ratio between the amplitude of a ship or floating structure motion, (whether translational or rotational) and the amplitude of the incident wave at a given wave frequency [19] [21]. This ratio provides a concise yet comprehensive means of characterizing the vessel's linear response to harmonic wave excitation.

Since the RAO varies with frequency, it enables the assessment of resonance phenomena, identification of frequency ranges associated with amplified or attenuated motions and comparison of predicted responses under different loading conditions or hull configurations. In practical terms, RAOs form foundation for estimating ship or floating structure motions in irregular water ways through spectral methods, as they allow the motion spectrum to be obtained by combining the RAO with the wave energy spectrum. Mathematically RAO can be expressed as follows

$$RAO = \frac{\theta_0}{K_\omega \zeta_0} = \frac{\theta_0}{(\omega^2/g)\zeta_0} \tag{5}$$

Maxsurf Motions applies a frequency-domain strip-theory formulation based on linear potential flow theory. Hydrodynamic coefficients, including added mass, radiation damping, and wave excitation forces, were internally generated by the software as functions of encounter frequency. The analysis assumes small-amplitude motions, incompressible fluid flow and negligible viscous effects, consistent with conventional linear seakeeping theory. Boundary conditions were defined as unrestricted floating-body motions in calm-water equilibrium prior to wave excitation. The simulation considered six-degree-of-freedom rigid body motion responses, with particular attention given to heave, pitch and roll motions due to their operational relevance for floating dock operations.

Ultimately, seakeeping analysis was done to enhance operation comfort and decreasing the motions of the floating structure arising from the wave – current interaction in the water area. Especially for the floating rigid dock designed using recycled plastic jerry can – pontoon like in this study, seakeeping becoming a very essential analysis due to its unique floats material combination. Thus, this analysis can help in finding the most optimum floating rigid dock model which suitable to be utilized in the designated area.

3. Results and Discussions

Based on the data collected from the field observation and the design of the floating rigid dock being created, several results can be exhibited. Although the seakeeping analysis focused on the motions of floating structures, hydrostatic calculation still need to be carried out to provide the initial conditions of each model which going to be simulated. Hence, the results of calculations and simulations can be presented as follows.

3.1. Hydrostatic Calculation

Hydrostatics provides a quantitative characterization of the form and properties of a vessel and/or floating structure, expressed in terms of the interactions between the structure and its surrounding water area. This analysis is primarily concerned with the forces exerted by water pressure on fully or partially submerged structures, and the consequent effects of these forces on the behavior of the floating structure, with particular emphasis on its buoyancy. The hydrostatic calculations were entirely performed using Maxsurf: Modeller following the completion of the 3D models for each floating rigid dock design. Fundamentally, Archimedes' principle underpins the hydrostatic analysis: the buoyant force acting on a structure is equal to the weight of the water displaced by the submerged portion of the structure. In the context of offshore structures, the equilibrium between the buoyant force and the total weight of the structure determines whether the structure can float stably. Based on the simulated model, the results can be presented as follows:

Table 2. Hydrostatic of Floating Rigid Dock Base Model

Measurement	Value	Unit
Displacement	750.1	kg
Volume (displaced)	750121251.0	mm^3
Draft Amidships	356.0	mm
Immersed depth	356.0	mm
WL Length	2600.0	mm
Beam max extents on WL	840.0	mm
Wetted Area	12151283.1	mm^2
Max sect. area	297002.0	mm^2
Waterpl. Area	2121668.4	mm^2
Prismatic coeff. (Cp)	0.971	
Block coeff. (Cb)	0.965	
Max Sect. area coeff. (Cm)	0.993	
Waterpl. area coeff. (Cwp)	0.971	
LCB length	1300.0	from zero pt. (+ve fwd) mm
LCF length	1300.0	from zero pt. (+ve fwd) mm
LCB %	50.000	from zero pt. (+ve fwd) % Lwl
LCF %	50.000	from zero pt. (+ve fwd) % Lwl
KB	179.2	mm
KG fluid	0.0	mm
BMt	166.1	mm
BML	1594.3	mm
GMt corrected	345.2	mm
GML	1773.4	mm
KMt	345.2	mm
KML	1773.4	mm

Measurement	Value	Unit
Immersion (TPc)	0.021	ton/cm
MTc	0.005	ton.m
RM at 1deg = GMt.Disp.sin(1)	4519.4	kg.mm
Length:Beam ratio	3.095	
Beam:Draft ratio	2.360	
Length:Vol^0.333 ratio	2.862	

Hydrostatic data vary according to the shape of the structure and the extent of the submerged area of the floating structure, in accordance with Archimedes' principle. This is evident from the displacement values of each floating dock model, with the largest displacement observed in the U-shaped model due to its greater wetted surface area (WSA) compared to the other designs, and its maximum load draft measured at the midship point (Draft Amidships). In this simulation, the floating docks were assumed to be in an even-keel condition, with both the bow and stern longitudinal lines levelled, resulting in identical vertical centre of buoyancy (KB) values for all models.

Table 3. Hydrostatic of Floating Rigid Dock U-Shape Model

Measurement	Value	Unit
Displacement	1667	kg
Volume (displaced)	1667268323.8	mm^3
Draft Amidships	356.0	mm
Immersed depth	356.0	mm
WL Length	2600.0	mm
Beam max extents on WL	2521.2	mm
Wetted Area	27002850.2	mm^2
Max sect. area	891433.3	mm^2
Waterpl. Area	4715772.9	mm^2
Prismatic coeff. (Cp)	0.719	
Block coeff. (Cb)	0.714	
Max Sect. area coeff. (Cm)	0.993	
Waterpl. area coeff. (Cwp)	0.719	
LCB length	1199.2	from zero pt. (+ve fwd) mm
LCF length	1199.2	from zero pt. (+ve fwd) mm
LCB %	46.122	from zero pt. (+ve fwd) % Lwl
LCF %	46.122	from zero pt. (+ve fwd) % Lwl
KB	179.2	mm
KG fluid	0.0	mm
BMt	1964.9	mm
BML	1703.9	mm
GMt corrected	2144.1	mm
GML	1883.0	mm
KMt	2144.1	mm
KML	1883.0	mm
Immersion (TPc)	0.047	ton/cm
MTc	0.012	ton.m
RM at 1deg = GMt.Disp.sin(1)	62388.9	kg.mm
Length:Beam ratio	1.031	
Beam:Draft ratio	7.082	
Length:Vol^0.333 ratio	2.193	

However, when considered longitudinally, differences arise due to the varying principal dimensions of the floating rigid docks. This not only affects the longitudinal center of buoyancy (LCB) but also influences the block coefficient (Cb). As shown in Tables 1, 2, and 3, the T-shaped model exhibits the lowest block coefficient, as its form deviates most significantly from a rectangular block shape. The block coefficient (Cb) represents the ratio between the volume of the vessel or floating structure and that of a rectangular block of the same overall length, breadth and draught. Thus, the closer shape is to a rectangular block, the nearer the Cb value approaches 1.0, which represents the maximum possible value.

Table 4. Hydrostatic of Floating Rigid Dock T-Shape Model

Measurement	Value	Unit
Displacement	1082	kg
Volume (displaced)	1081506331.9	mm^3
Draft Amidships	356.0	mm
Immersed depth	356.0	mm
WL Length	2600.0	mm
Beam max extents on WL	2520.0	mm
Wetted Area	17551853.5	mm^2
Max sect. area	891006.1	mm^2
Waterpl. Area	3058965.7	mm^2
Prismatic coeff. (Cp)	0.467	
Block coeff. (Cb)	0.464	
Max Sect. area coeff. (Cm)	0.993	
Waterpl. area coeff. (Cwp)	0.467	
LCB length	1610.9	from zero pt. (+ve fwd) mm
LCF length	1610.9	from zero pt. (+ve fwd) mm
LCB %	61.956	from zero pt. (+ve fwd) % Lwl
LCF %	61.956	from zero pt. (+ve fwd) % Lwl
KB	179.2	mm
KG fluid	0.0	mm
BMt	777.6	mm
BML	1748.3	mm
GMt corrected	956.7	mm
GML	1927.4	mm
KMt	956.7	mm
KML	1927.4	mm
Immersion (TPc)	0.031	ton/cm
MTc	0.008	ton.m
RM at 1deg = GMt.Disp.sin(1)	18058.2	kg.mm
Length: Beam ratio	1.032	
Beam: Draft ratio	7.079	
Length: Vol^0.333 ratio	2.533	

This is directly related to the prismatic coefficient (Cp) and the water-plane area coefficient (Cwp), whereby the closer the shape of the structure approaches the reference geometry – namely a prism for Cp and a rectangle or square for Cwp – the higher the respective coefficient values.

3.2. Response Amplitude Operator (RAO)

In evaluating and analyzing the seakeeping performance of the floating rigid dock, numerous factors influence its behavior, including wave height, current, weather conditions, water flow velocity, frequency and wave approach angle (angle of attack) as external factors, as well as the dock's geometry, draft and payload as internal factors. For the present study, seakeeping analysis was conducted using computer simulations, Maxsurf: Motions. In the simulation, tidal wave heights, wave angle of attacks, and current velocities were based on field measurements, while the wave spectrum was represented using JONSWAP spectrum. This spectrum was selected because the floating rigid dock operates in an open-water environment where waves are irregular, never reaching fully developed conditions, and continue to evolve as wind speed increases with changing weather.

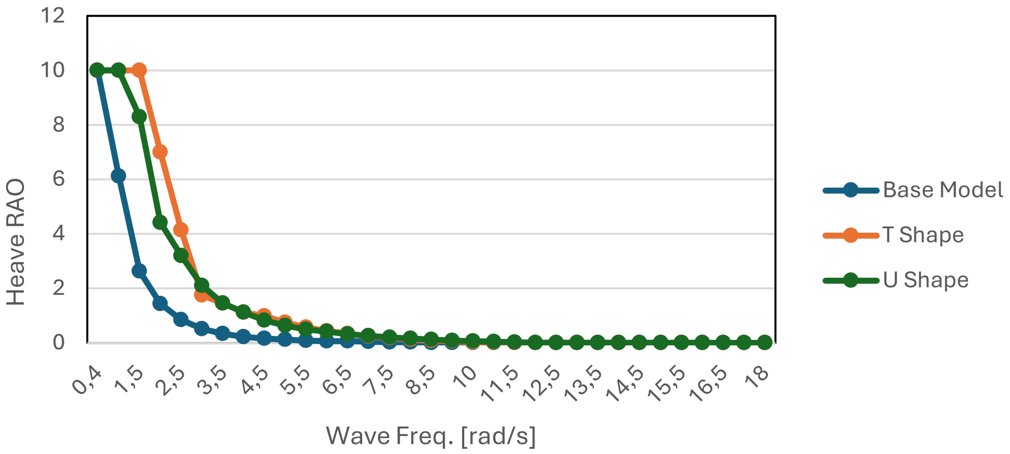

Figure 6. Heave Motions in 90 deg. angle of attack (Beam Sea)

According to the designated location for the floating rigid dock construction (as shown in Figure 2), situated in a river estuary opening to the sea, the water flow approaches predominantly from a single direction, namely 90 deg (Beam Sea) relative to the dock's orientation. However, to provide a more detailed assessment of the dock's seakeeping performance, additional simulations were also conducted for a 180 deg wave angle of attack (Head Sea).

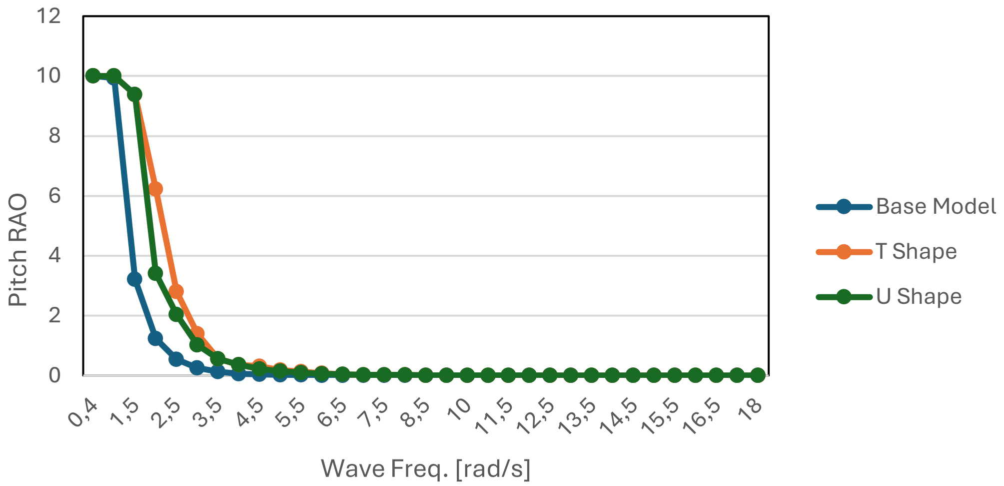

Figure 7. Pitch Motion in 90 deg. angle of attack (Beam Sea)

Following the simulations and analysis at a wave approach angle of 90 deg (Beam Sea), the T-shaped model exhibited the highest heave and pitch motion intensities, whereas the Base Model showed the lowest (Figure 4 and 5). This behavior is attributed to the differing bow and stern configurations of the T-shaped model, resulting in an uneven weight distribution, with the bow being heavier than stern. Consequently, the stern is more readily to be lifted when the dock encounters upward wave forces. Moreover, the heavier bow of the T-shaped model causes the bow to descend more rapidly into the wave through after passing the wave crest.

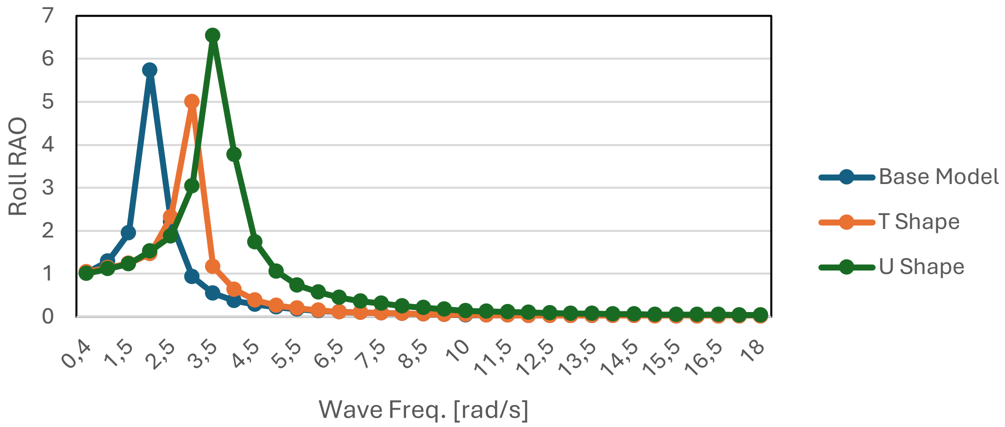

Figure 8. Roll Motion in 90 deg. angle of attack (Beam Sea)

For roll motion, the U-shaped model exhibited the highest intensity, while the Base Model remained the lowest (Figure 6). Unlike heave and pitch, the T – shaped model displayed lower roll intensity than the U – shaped model, as the latter's configuration results in a greater concentration of mass along the port and starboard sides. Furthermore, this shape (see Figure 3) facilitates the transfer of wave forces from one side to the other, thereby amplifying roll motion in the floating dock. In addition, the larger wetted-surface area (WSA) of the structure contributes to increased motion intensity. Structures with larger WSA experience more significant interactions with the surrounding fluid, resulting in greater dynamic responses compared to structures with smaller wetted areas.

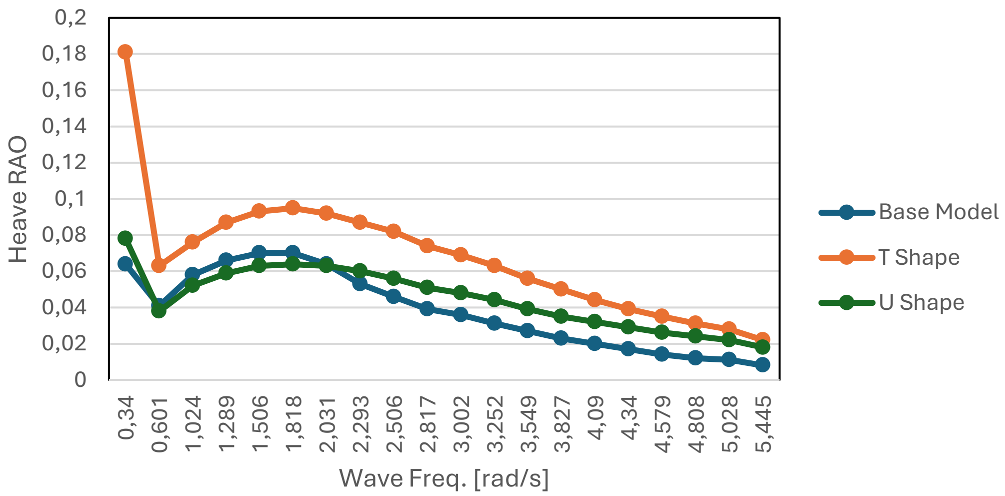

Figure 9. Heave Motions in 180 deg. angle of attack (Head Sea)

In the seakeeping analysis at a wave angle of attack of 180 deg (Head Sea), the floating rigid dock's motion simulations produced results broadly similar to those observed at 90 deg (Beam Sea). However, differences in motion patterns were still evident due to the change in wave direction, which alters the interaction between the dock and the fluid waves. In heave motion (Figure 8) at 180 deg (Head Sea), the motion pattern exhibited more pronounced fluctuations compared with 90 deg (Beam Sea). This behavior arises from the differing interaction mechanisms: in Head Sea, wave translation impacts the dock longitudinally, whereas in Beam Sea, the interaction is predominantly transverse, with waves striking the dock from the port or starboard sides.

Among the investigated configurations, the T-shaped floating dock provides the most balanced engineering performance. Although the U-shaped model exhibits the highest transverse stability (GMt = 2.144 m) and displacement capacity (1.667 kg), it also generates the largest roll response under beam-sea conditions due to its wider lateral mass distribution and larger wetted surface area. Excessive roll motion may reduce user comfort and operational safety during boarding and unloading activities. Conversely, the Base model demonstrates the lowest motion responses but provides the smallest displacement capacity (750 kg), limiting its practical usefulness for multi-vessel operations. The T-Shaped configuration represents an intermediate solution, offering a displacement capacity approximately 44% greater than the Base model while maintaining lower roll responses than the U-shaped configuration. This combination of adequate payload capacity, improved berthing functionality, and moderate motion characteristics makes the T-shaped configuration the most suitable alternative for estuarine floating dock applications.

The factors causing one model to exhibit higher motion intensity than others at a wave angle of attack in 180 deg (Head Sea) are largely the same as those at 90 deg (Beam Sea). However, unlike Beam Sea, which induces heave, pitch, and roll, Head Sea conditions do not generate roll motion, as there is no transverse interaction between the waves and the floating rigid dock. Consequently, under Head Sea conditions, only translational motions are excited, while rotational motions remain minimal or absent.

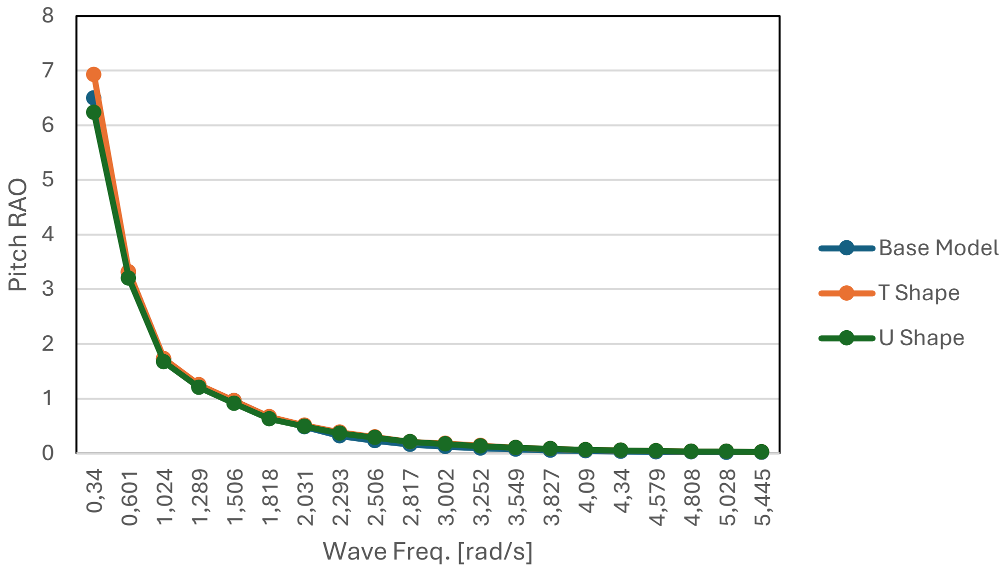

Figure 10. Pitch Motions in 180 deg. angle of attack (Head Sea)

Based on the seakeeping analysis and simulation results, taking into account other variables such as design, capacity, and ease of on-site installation, the T-shaped floating dock model was selected for implementation. This because the T-shaped model exhibits lower roll intensity compared with the U-shaped model, facilitating safer and more stable footing on the deck when boarding vessels. Additionally, the T-shaped design is more compatible with the topography of the installation area, allowing the existing site conditions to be utilized without requiring widening or dredging. Compared with the Base Model, the T-shaped dock offers greater berthing capacity due to its wider bow, accommodating more vessels simultaneously. Although the T-shaped model experiences higher heave motion than the other models, this drawback can be mitigated through the use of mooring devices, such as anchors or ropes secured to the shoreline.

From a practical perspective, the proposed floating dock system offers a low-cost infrastructure alternative for coastal and estuarine communities where access to conventional port facilities is limited. The utilization of recycled plastic jerry cans significantly reduces material costs while simultaneously providing a productive reuse pathway for plastic waste. This approach supports circular-economy principles and may assist local governments and community organizations in developing affordable waterfront infrastructure for a small fishing vessel, community transport, and environmental monitoring activities.

Moreover, the floating nature of the dock enables adaptation to tidal fluctuations and seasonal water-level variations, making it particularly suitable for river-mouth settlements and flood-prone coastal areas where fixed structures may be less effective or more expensive to construct. The modular arrangement of recycled plastic jerry-can pontoons also provides considerable scalability potential. Because the buoyancy elements are independent and easily assembled, the dock dimensions can be adjusted according to operational requirements without substantial changes to the overall construction concept. Additional modules may be incorporated to accommodate larger vessel capacities, increased payload demands or expanded community facilities. Consequently, the proposed design framework can be adapted for applications ranging from small fishing villages to larger community-based waterfront developments, particularly in developing regions where cost efficiency remains a primary consideration.

3.3. Numerical Reliability and Limitations

The dynamic behavior of the floating rigid dock was evaluated through Response Amplitude Operator (RAO) analysis. The RAO represents the ratio between motion amplitude and incident wave amplitude as a function of encounter frequency and is widely used to assess the seakeeping performance of floating structures. For each dock configuration, RAOs were calculated for heave, pitch, and roll motions under beam-sea (90°) and head-sea (180°) wave conditions. The resulting RAO curves were analyzed to identify dominant motion responses and critical frequency regions associated with amplified structural motions.

The seakeeping simulations were performed using Maxsurf Motions, which applies a frequency-domain strip-theory approach based on linear potential-flow assumptions. This numerical formulation has been widely adopted for the preliminary hydrodynamic assessment of ships and floating structures and is considered suitable for evaluating relative differences in motion responses among alternative configurations. The observed motion trends are physically consistent with established seakeeping theory, whereby wave excitation forces, restoring moments, and geometric characteristics govern the resulting motion amplitudes.

The present study is intended as a preliminary numerical investigation of floating rigid dock performance utilizing recycled plastic jerry-can pontoons. Experimental measurements and full-scale field validation were beyond the scope of the present study and therefore were not conducted. Consequently, the results should be interpreted primarily as a comparative assessment of alternative dock configurations rather than absolute operational performance estimates. Nevertheless, since all models were analyzed using identical environmental conditions, hydrodynamic assumptions, and computational procedures, the results provide a consistent basis for configuration comparison and preliminary design selection.

The numerical approach employed in this study is consistent with the methodology previously applied by Poundra et al. (2017,2024), who utilized Maxsurf Motions and frequency-domain RAO analysis to evaluate the hydrodynamic performance of alternative hull configurations. Similar to their findings, the present study demonstrates that modifications in geometry alter the hydrodynamic characteristics of the structure, leading to measurable differences in heave, pitch, and roll responses across the investigated frequency range. Therefore, the observed trends may be considered physically reasonable and consistent with previous seakeeping studies employing frequency-domain motion analysis. Future work should include physical model experiments or full-scale monitoring to further verify the predicted motion responses under actual environmental conditions.

5. Conclusions

This study numerically evaluated the hydrostatic characteristics and seakeeping performance of modular floating rigid dock configurations employing recycled 30-L HDPE plastic jerry cans as buoyancy modules for estuarine applications. The results demonstrated that the pontoon arrangement significantly influenced the hydrostatic properties and motion characteristics of the floating dock. Compared with the Base configuration, the T-shaped and U-shaped models increased displacement by approximately 44.3% and 122.3%, respectively, while the U-shaped configuration achieved the highest transverse metacentric height (GMt = 2.144 m), indicating superior initial transverse stability.

The frequency-domain seakeeping analysis revealed that variations in pontoon configuration had only a minor influence on the heave and pitch responses, with differences generally remaining below 10% under the investigated wave conditions. Conversely, the transverse arrangement of the buoyancy modules substantially affected the roll response, where the T-shaped configuration reduced the peak roll response amplitude operator (RAO) by approximately 23% compared with the U-shaped configuration. These results indicate that the geometric arrangement of buoyancy modules primarily governs the transverse motion performance, whereas the vertical motion characteristics remain relatively insensitive to the investigated configurations under moderate wave conditions.

Considering hydrostatic capacity, motion response, operational functionality, and construction practicality, the T-shaped configuration exhibited the most balanced overall performance for estuarine floating dock applications. The study further demonstrates that recycled HDPE plastic jerry cans can be effectively utilized as sustainable and economical buoyancy modules for modular floating dock systems, providing a technically feasible alternative for small-scale waterfront infrastructure.

The present investigation is limited to numerical simulations based on linear strip-theory hydrodynamics implemented in Maxsurf Motions. Therefore, future research should include experimental validation through physical model tests or full-scale field measurements, together with investigations on structural strength, long-term durability, environmental degradation, and service-life performance of recycled plastic buoyancy modules under actual operating conditions.

Acknowledgment

The authors would like to express their sincere gratitude to all individuals and institutions who contributed to the successful completion of this research. We extended our appreciation to Universitas Hang Tuah and Universitas Katolik Widya Mandala Surabaya for providing the necessary facilities and support throughout the study. Special thanks are also due to the field team for their assistance in data collection and the technical staff for their guidance in the utilization of Maxsurf simulation software.

We are particularly grateful to the Indonesia Ministry of Higher Education, Science and Technology for their financial support, which made this research possible. Finally, we acknowledge the valuable insights and constructive feedback from colleagues and reviewers, which greatly improved the quality of this work.

References

[1] H. B. D. Paul, "Wave attenuation on a floating rigid dock by multiple surface-piercing vertical thin perforated barriers," *Engineering Analysis with Boundary Elements,* vol. 169, no. 105985, 2024.

[2] M. C. O. X. W. Jianan Zhang, "Dynamic and Structural analyses of floating dock operations considering dock-vessel coupling loads," *Ocean Engineering,* vol. 310, no. 118622, 2024.

[3] R. Y. Z. G. P. C. S. Zhiyu Jiang, "Design, modelling, and analysis of a large floating dock for spar floating wind turbine installation," *Marine Structures,* vol. 72, no. 102781, 2020.

[4] S. K. D. S. K. Kailash Chand Swami, "Water waves scattering by floating rigid dock and breakwaters using improved singular boundary method under regular and irregular waves," *Results in Engineering,* vol. 25, no. 104420, 2025.

[5] J. L. Z. L. G. H. J. L. X. C. Song Ji, "Numerical and experimental study on motion responses of hinged multiple floating bodies with damaged bottom openings," *Ocean Engineering,* vol. 359, no. 125964, 2026.

[6] L. Q. M. L. J. L. Z. L. Y. M. C. A. Zhangjian Wang, "Experimental investigation on the motion responses of a moored outfitting ship with and without pontoons under extreme conditions," *Ocean Engineering,* vol. 343, no. 123434, 2026.

[7] N. S. Q. S. J. L. Peixiu Chen, "Under net-zero ambitions and decent living standards: Turning to a regional synergistic plastic waste management system from the linear system," *Environmental Impact Assessment Review,* vol. 120, no. 108472, 2026.

[8] N. S. E. W. Hilyatun Nuha, "An integrated optimization framework for reverse supply chain design in plastic waste management," *Supply Chain Analytics,* vol. 15, no. 100213, 2026.

[9] M. H. M. H. Masoud Ghaffari, "Life cycle assessment of the healthcare plastic waste management in Finland, a case study: HUS Meilahti hospital area," *Waste Management,* vol. 218, no. 115528, 2026.

[10] J. L. J. X. L. C. M. B. Haoran Liu, "Bridging science and policy towards integrated management of Urban plastic pollution: A global review of patterns, drivers, and solutions," *Environmental Impact Assessment Review,* vol. 118, no. 108323, 2026.

[11] M. A. A. R. N. D. M. K. A. K. D. H. E. N. H. M. M. H. D. W. M. R. B. Handyastono, "Flood hazard assessment in Pemaluan Village due to land use change in IKN (Ibu Kota Nusantara) as the New Capital City of Indonesia," *Case Studies in Chemical and Environmental Engineering,* vol. 11, 2025.

[12] M. B. K. E. O. N. M. B. A. Faiz Isma, "Flood hazard assessment in Kuala Langsa village, Langsa city, Aceh Province-Indonesia," *Case Studies in Chemical and Environmental Engineering,* vol. 10, 2024.

[13] X. F. A. K. Y. N. A. Z. Yi-bin Xiao, "Port investments on coastal and marine disasters prevention: Economic modeling and implications," *Transportation Research Part B: Methodological,* vol. 78, pp. 202 - 221, 2015.

[14] C. B. Barrass, Ship Design and Performance for Masters and Mates, Oxford: Elsevier Butterworth-Heinemann, 2004.

[15] B. K. A. S. W. G. A. P. Poundra, "Hydrodynamic Force Comparison on Multi-Hull, Monohull and Single-to-Twin After Ship Hull (STASH) Based on Seakeeping Criteria," *IPTEK The Journal of Engineering,* pp. 205-229, 2024.

[16] I. K. A. P. U. D. H. B. S. G. A. P. Poundra, "Optimizing Trimaran Yacht Hull Configuration Based on Resistance and Seakeeping Criteria," *Procedia Engineering,* vol. 194, pp. 112-119, 2017.

[17] W. O. W. K. Jungeun Kim, "A Numerical Study on the Seakeeping Performance and Ride Comfort of a Small MonoHull Vessel With and Without Hydrofoil in Regular Head Seas," *Journal of Marine Science and Engineering,* vol. 13, no. 10, 2025.

[18] H. M. H. a. S. Saad-Eideen, "Image-Based Hybrid Neural Network Model for Naval Ship Wave Resistance Prediction," *Journal of Marine Science and Engineering,* vol. 14, no. 3, 2026.

[19] K. G. A. R. Marion Zu, "Seakeeping criteria revisited," *Ocean Engineering,* vol. 297, no. 116785, 2024.

[20] O. D. Ioannis P. Mitseas, "Stohastic seakeeping analysis of nonlinear ship rolling dynamics under non-stationary and irregular sea states," *Computers & Structures,* vol. 323, no. 108164, 2026.

[21] T. T. M. A. D. K. S. S. Gyeongseo Min, "Seakeeping analysis of a damaged ship using CFD," *Ocean Engineering,* vol. 362, no. 126200, 2026.

[22] B. J. L. S. S. K. E. K. Xu Han, "Validation of vessel seakeeping model tuning algorithm based on measurements at model scale," *Marine Structures,* vol. 80, no. 103083, 2021.

[23] R. Bhattacharya, Dynamics of Marine Vehicles, New York: John Wiley and Sons, 1978.